JOURNAL OF GEOPHYSICAL RESEARCH, VOL. 111, XXXXXX, doi:10.1029/2005JA011306, 2006

Solar flare signatures of the ionospheric GPS total electron content

J. Y. Liu,[1,2] C. H. Lin,[1] Y. I. Chen,[3] Y. C. Lin,[1] T. W. Fang,[1] C. H. Chen,[1] Y. C. Chen,[1] and J. J. Hwang[4]

Received 7 July 2005; revised 21 November 2005; accepted 17 January 2006; published XX Month 2006.

[1] In this study, ionospheric solar flare effects on the total electron content (TEC) and associated time rate of change (rTEC) derived from ground-based global positioning system (GPS) receivers in the midday region are examined. The occurrence times and locations of 11 solar flares are isolated from the 1–8 Å X-ray radiations of the geosynchronous operational environmental satellite (GOES) and the SOHO Extreme Ultraviolet Imaging Telescope (EIT) images, respectively, while the TEC and rTEC are obtained from the international GPS services (IGS). Results show that the maximum value of the TEC increase solely depends on the flare class, while the maximum value of the rTEC increase is related to not only the flare class but also the time rate of change in flare radiations. A statistical analysis further demonstrates that the two maximum values are inversely proportional to the cosine of the great circle angle between the center and flare locations on the solar disc.

Citation: Liu, J. Y., C. H. Lin, Y. I. Chen, Y. C. Lin, T. W. Fang, C. H. Chen, Y. C. Chen, and J. J. Hwang (2006), Solar flare signatures of the ionospheric GPS total electron content, *J. Geophys. Res.*, *111*, XXXXXX, doi:10.1029/2005JA011306.

1. Introduction

[2] Sudden ionospheric disturbances (SIDs) result from an interaction of solar flare radiations with constituents of the upper atmosphere, which form a major part of flare monitoring program in many observatories. The ionospheric solar flare effects or SIDs provide an interest in the reaction of the ionospheric plasma to an impulsive ionization [*Mitra*, 1974]. The disturbances have important effects on radio communications and navigations over the entire radio spectrum [*Davies*, 1990]. *Davies* [1990] reviewed that SIDs were generally recorded as the short wave fadeout [*Stonehocker*, 1970], sudden phase anomaly [*Jones*, 1971; *Ohshio*, 1971], sudden frequency deviation (or frequency shift; Doppler shifts) [*Donnelley*, 1971], sudden cosmic noise absorption [*Deshpande and Mitra*, 1972], sudden enhancement/decrease of atmospherics [*Sao et al.*, 1970], and sudden increase in total electron content (TEC) [*Mendillo et al.*, 1974; *Davies*, 1980]. In the early years, the most common technique to study the ionospheric solar flare effects is to examine Doppler (frequency) shift in signals transmitted by Doppler sounding systems. However, owing to the high-frequency band (HF, 3–30 MHz) [e.g. *Hunsucker*, 1991] used, the Doppler sounding system observation generally suffers from the short wave fadeout and often no data was recorded even during the midway of the flare occurrence [e.g., *Davies*, 1990; *Liu et al.*, 1996a].

[3] To simultaneously monitor a large area of the ionosphere response to solar flares, the global positioning system (GPS) is ideal to be employed. The system consists of more than 24 satellites, distributed in six orbital planes around the globe at an altitude of about 20,200 km. Each satellite transmits signals in two frequencies (f_1 = 1575.42 MHz and f_2 = 1227.60 MHz). Since the ionosphere is a dispersive medium, scientists are able to evaluate the ionospheric effects with measurements of the modulations on carrier phases and phase codes recorded by dual-frequency receivers [*Sardón et al.*, 1994; *Leick*, 1995; *Liu et al.*, 1996b]. Meanwhile, owing to the transmitted frequencies being much greater than the ionospheric collision frequencies, the ionospheric absorption (signal fadeout) effects for the GPS signals are minor. Scientists report global views of ionospheric solar flare effects by means of the GPS technique [*Zhang et al.*, 2002; *Zhang and Xiao*, 2003; *Liu et al.*, 2004]. *Liu et al.* [2004] proposed two GPS observed quantities, the TEC and its time rate of change (rTEC), for observing ionospheric solar flare effects. They found that ionospheric responses of the two quantities depend on the local time of observation (or hour angle) and the most pronounced solar flare effects are in the midday region. They further show theoretically that the rTEC stands for the frequency deviation of the GPS signals and is well correlated to Doppler shift in signals transmitted by Doppler sounding systems. Instead of the global view of a particular event, *Zhang et al.* [2002] examined several flare events and found that for the similar classes, flares occurring near the solar meridian result in stronger ionospheric responses.

[4] In this paper we examine TEC and rTEC variations in the midday region during ten X-class and one M-class solar flare events (Table 1), including the greatest flare of class

[1]Institute of Space Science, National Central University, Chung-Li, Taiwan.
[2]Also at Center for Space and Remote Sensing Research, National Central University, Chung-Li, Taiwan.
[3]Institute of Statistics, National Central University, Chung-Li, Taiwan.
[4]Science Education Department, National Museum of Natural Science, Tai-Chung, Taiwan.

0148-0227/06/2005JA011306$09.00

Table 1. Parameters of the 11 Solar Flare Events[a]

Date	DOY	Flare Class	Start, hhmm	Maximum, hhmm	End, hhmm	Active Region	α Angle, deg	Increase Rate, Watt/m²s
2003/11/04	308	X28	1929	1950	2206	S19 W83	86.136	0.0314
2001/04/02	092	X20	2132	2151	2203	N16 W56	58.637	0.0074
2003/10/28	301	X17.2	0951	1110	1124	S16 E08	17.912	0.0140
2001/04/15	105	X14.4	1319	1350	1355	S22 W72	76.338	0.0213
2003/10/29	302	X10	2037	2049	2101	S15 W02	15.134	0.0082
2003/11/02	306	X8.3	1703	1725	1739	S14 W56	58.029	0.0054
2000/07/14	196	X5.7	1003	1024	1043	N17 E03	17.267	0.0031
2002/07/23	204	X4.8	0018	0035	0047	S13 E72	73.538	0.0044
2002/07/03	184	X1.5	0208	0213	0216	S18 W51	54.523	0.0037
2004/02/26	057	X1.1	0150	0203	0210	N14 W15	20.574	0.0009
2004/11/06	311	M9.3	0011	0034	0042	N09 E06	10.824	0.0266

[a]Time is in Universal Time.

X28 occurring on 4 November 2003 and the well-known, fourth-greatest flare of class X17.2 on 28 October 2003, the so-called Halloween flare and storm, to find the relationship between the two quantities and the flare locations on the solar disc. Meanwhile, simultaneous observations from ground-based GPS receivers and a Doppler sounding system colocated in Taiwan during an M9.3 flare are examined to find whether the frequency deviations (or Doppler shifts) of the two transmitted signals show similar tendencies as suggested by *Liu et al.* [2004].

2. Observation

[5] For a Doppler sounding system, the frequency deviation Δf_D from the operating (or transmitting) frequency f is proportional to the rate of change of phase path of the signal and is given by [*Bennett*, 1967]

$$\Delta f_D = -\frac{f}{c}\int_{Tx}^{Rx}\frac{\partial\mu}{\partial t}\cos\alpha ds = -\frac{f}{c}\int_{Tx}^{Rx}\frac{\partial\mu}{\partial N}\frac{\partial N}{\partial t}\cos\alpha ds, \quad (1)$$

where μ is phase refractive index and α is the angle between the wave normal and the ray direction. Tx and Rx denote the transmitter and receiver antennas. Here c is light speed in free space, N represents the ionospheric electron density, and s denotes the integration along the radiowave path from Tx to Rx. Since $d\mu/dN$ is a negative quantity, Δf_D is then proportional to dN/dt.

[6] In practice, flare radiations, often with a broad spectrum, ionize the whole ionosphere and enhance the electron density within it, which also results in altitude descending of the reflection point P_R of signals transmitted by a Doppler sounding system. Thus equation (1) can be rewritten as

$$\Delta f_D = -\frac{f}{c}\int_{Tx}^{Rx}\frac{\partial\mu}{\partial t}\cos\alpha ds = -\frac{f}{c}\left[\int_{Tx}^{P_R}\frac{\partial\mu}{\partial t}\cos\alpha ds + \int_{P_R}^{Rx}\frac{\partial\mu}{\partial t}\cos\alpha ds\right] \quad (2)$$

Note that the P_R descending means the phase paths between Tx and P_R as well as P_R and Rx being shorten, which in turn gives the Δf_D to be positive (increased).

[7] On the other hand, *Liu et al.* [2004] proposed that the two quantities, the TEC and its time rate of change, rTEC, observed by ground-based GPS receivers, can be employed to monitor the ionospheric solar flare effects. The two quantities can be stated as

$$TEC = \cos\chi\int_{Sat}^{Rx} Nds \quad (3)$$

$$rTEC = \frac{\partial TEC}{\partial t} \cong \frac{cf\,\Delta f_{GPS}}{40.3} \quad (4)$$

where χ is the zenith angle of the GPS satellite at a GPS receiving station Rx. On the basis of equation (4), the frequency shift of the GPS signal Δf_{GPS} in Hz can be expressed as

$$\Delta f_{GPS} \cong \frac{40.3}{cf}\frac{\partial TEC}{\partial t} = 0.032\frac{\partial TECu}{\partial t}, \quad (5)$$

where $dTECu/dt$ is in TECu/sec (1 TECu = 10^{16} el/m^2).

[8] To validate the relationship between equations (2) and (5), a concurrent observation of a Doppler sounding system and GPS receivers in Taiwan is carried out. The operation frequency of the Doppler sounding system is 5.262 MHz and the distance between the transmitter at Liyutan (24.3°N, 120.8°E) and the receiver at National Central University (25.0°N, 121.2°E) is about 80 km. We assume the reflection point P_R of the 5.262 MHz signals to be 200 km altitude, and the incidence angle is about 11°. Thus the Doppler sounding system performs a nearly vertical probing.

3. Result and Interpretation

[9] To avoid the local time (solar zenith angle) effects, the GPS TEC and rTEC observed around the midday regions are used to examine the ionospheric responses to ten X-class and one M-class flares occurred at various locations on the solar disc. The occurrence time and location (see Table 1) as well as X-ray radiations in 1–8 Å with 1-min time resolution of each event are observed by sweeping the solar with the X-ray sensor on the geosynchronous operational environmental satellite (GOES). The midday TEC and rTEC are derived from ground-based receivers of the international GPS service (IGS) and the Taiwan network.

[10] Figure 1 illustrates the SOHO Extreme Ultraviolet Imaging Telescope (EIT) images of the fourth largest flare

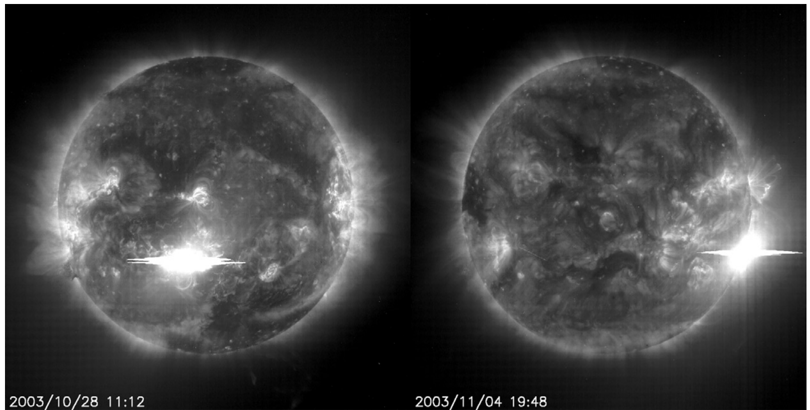

Figure 1. SOHO Extreme Ultraviolet Imaging Telescope (EIT) images of the fourth largest on 28 October 2003 (left) and the largest solar flare on 4 November 2003 (right).

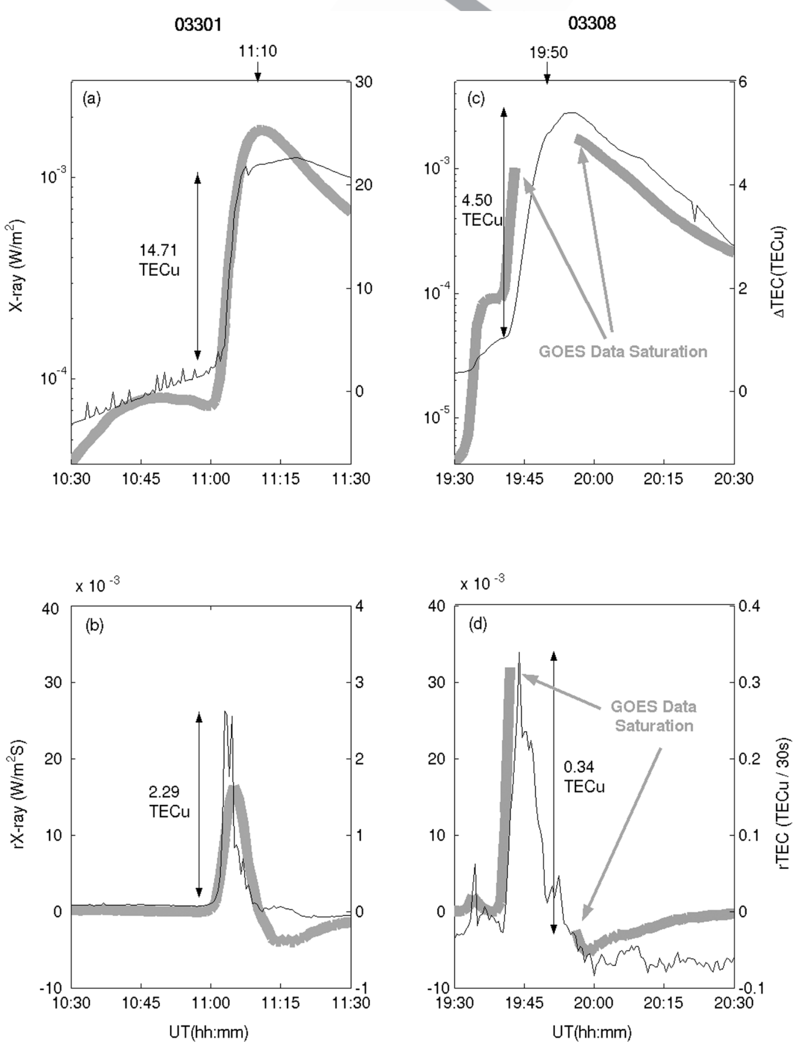

Figure 2. The 1–8 Å solar X-ray radiations from GOES (bold gray curves and left axes) and ionospheric GPS TEC (dark curves and right axes) responses to flares. (a) X-ray (gray curve) and TEC (dark curve) as well as (b) rX-ray (gray curve) and rTEC (dark curve) variations on 28 October 2003 (03301). (c) X-ray and TEC as well as (d) rX-ray and rTEC variations on 4 November 2003 (03308). Note that the GOES data show data gaps/saturations during the 4 November 2003 flare.

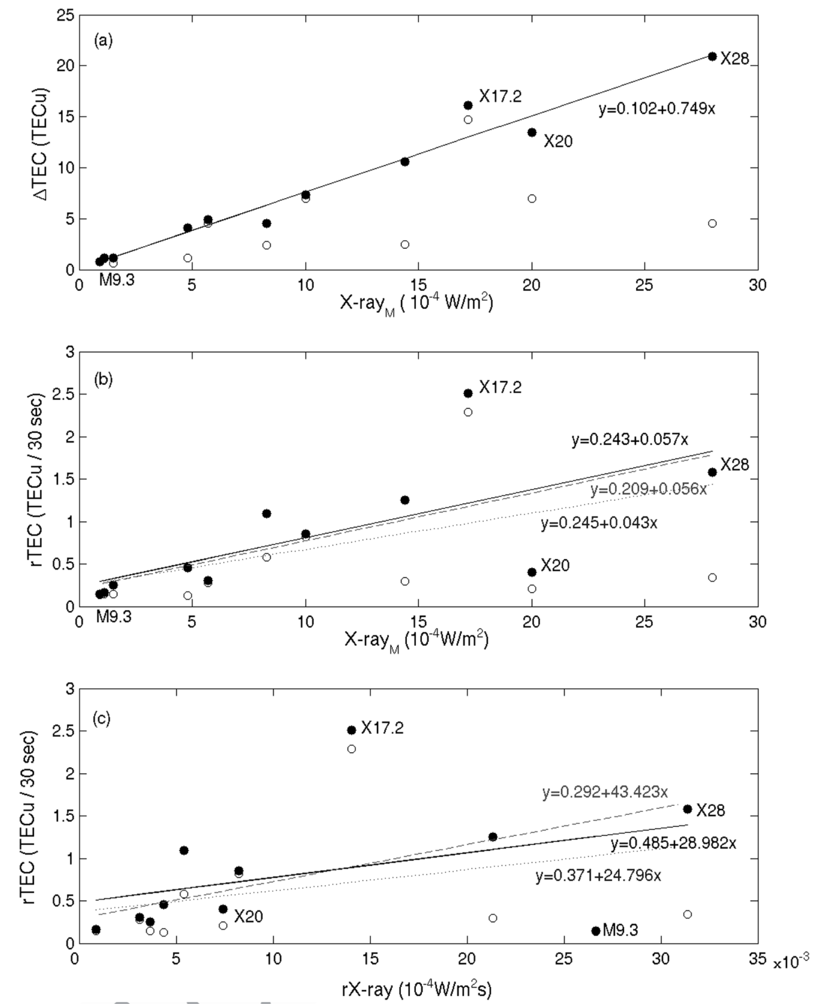

Figure 3. The maximum values of the flare 1–8 Å X-ray radiations and ionospheric TEC responses. (a) ΔTEC_M (open circles) and ΔTEC_{MC} (dots) versus X-ray$_M$, (b) $rTEC_M$ (open circles) and $rTEC_{MC}$ (dots) versus X-ray$_M$, and (c) $rTEC_M$ (open circles) and $rTEC_{MC}$ (dots) versus rX-ray$_M$. The calibrated data are fitted with the linear regression (lines). The dashed lines in Figures 3b and 3c represent the regression fitting lines using the whole data set, and the dotted lines represent the fitting lines without the outlier data point, the X17.2 flare. The solid lines represent the fitting lines without outlier and influential data points, the X20 flare in Figure 3b and the M9.3 flare in Figure 3c.

of class X17.2 appearing at (S16, E08), near the solar meridian, on 28 October (Halloween flare) 2003 and the largest flare of class X28 occurring at (S19, W83), around the edge of the solar disc, on 4 November 2003.

[11] Figure 2 shows that temporal variation in the increase TEC change ΔTEC and X-ray as well as those in rTEC and rX-ray are well correlated, respectively. It is surprised to find in Figure 2 that the maximum value 14.71 TECu of the TEC increase (ΔTEC_M) of the X17.2 flare is much greater than that 4.50 TECu of the X28 (Figures 2a and 2c). Similarly, in Figures 2b and 2d, while the X28 has a greater value in the maximum time rate of change of the X-ray radiations, rX-ray$_M$ (31.4 versus 14.0 mWatt/m^{2}s), the X17.2 yields a greater value in the maximum time rate of change of the TEC, $rTEC_M$ (2.29 versus 0.34 TECu/30s). To resolve this puzzle, we further examine ΔTEC_M versus flare class (or X-ray$_M$), $rTEC_M$ versus flare class, and $rTEC_M$ versus rX-ray$_M$ for all the events (Figures 3a, 3b, and 3c). The open circle symbols in Figures 3a–3c show that the ΔTEC_M and $rTEC_M$ of the X17.2 flare occurred on 28 October yield the greatest values but show no clear relationship with X-ray radiations. It is noted that Figures 1 and 2 imply the flare location on the solar disc to be important. We therefore take into account the angle θ of the great circle from the center of the solar disc to the flare location and calibrate the two quantities as

$$\Delta TEC_{MC} = \Delta TEC_M / \cos\theta \qquad (6)$$

and

$$rTEC_{MC} = rTEC_M / \cos\theta \qquad (7)$$

The dotted symbols show that the calibrated quantities ΔTEC_{MC} and $rTEC_{MC}$ are generally well correlated with the flare radiations (X-ray$_M$) and time rate of change in X-ray

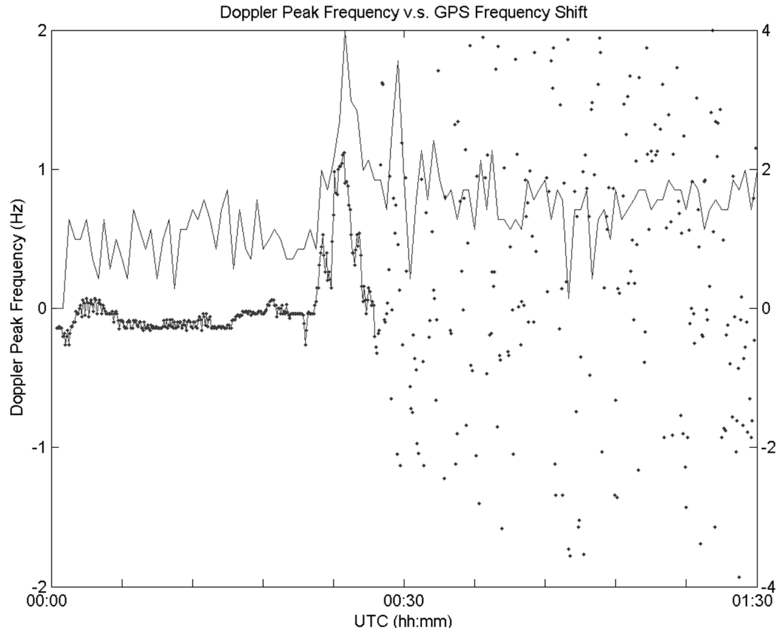

Figure 4. The frequency shifts simultaneously observed by the ground-based GPS receivers (solid curve) and Doppler sounding system (dots and dotted curve) in Taiwan for the M9.3 flare occurring on 26 February 2003.

(rX-ray$_M$), except for the rTEC$_{MC}$ values of the X17.2 and X20 flares shown in Figure 3b and for the X17.2 and M9.3 flares shown in Figure 3c. Note that the ΔTEC of the X20 flare and the rTEC of the M9.3 flare are much less than their associated predications (solid lines), while the ΔTEC and rTEC of the X17.2 flare are much greater than their predications (Figure 3b and 3c).

[12] The flare-produced frequency shifts have been simultaneously observed by the ground-based GPS receivers and Doppler sounding system in Taiwan since 2003. Because the Doppler sounding system generally suffers from the short wave fadeout significantly during X class flares, we focus on the two frequency shifts observed during an M9.3 flare occurred on 26 February 2003. It is found from Figure 4 that the two frequency shifts are generally well correlated to each other until the Doppler sounder observation encountered the short wave fadeout after about 0028 UT.

4. Discussion and Conclusion

[13] Results shown in Figure 2 confirm that the TEC is suitable to monitor the overall variations of flare radiations, and the rTEC is useful to depict the rate of change of flare radiations. The good agreement between the simultaneous measurements of the ground-based GPS TEC and the Doppler sounding system indicates that the rTEC stands for the Doppler frequency shift of the GPS signals (Figure 4).

[14] *Donnelly* [1976] and *Tsurutani et al.* [2005] find the strong center-to-limb effects in the solar flare EUV spectra. To see if the X-ray flare radiation is also anisotropic (the center-to-limb effect), we examine ΔTEC$_{MC}$ versus flare class (or X-ray$_M$), rTEC$_{MC}$ versus flare class, and rTEC$_{MC}$ versus rX-ray$_M$ for all the events (Figures 3a, 3b, and 3c).

[15] The regression analysis for the eleven pairs of data (x:flare class in X-ray radiations, y:ΔTEC$_{MC}$) indicates that 96.38% of the variation of the ΔTEC$_{MC}$ can be explained by the fitted regression line ΔTEC$_{MC}$ = 0.102 + 0.750 X-ray (Figure 3a). Moreover, applying the Fisher's z-transformation [*Kendall et al.*, 1977], we have the 95% confidence interval for the correlation coefficient between flare class and ΔTEC$_{MC}$ of (0.943, 0.994), which shows a strong linear association between the two quantities. The strong linear association demonstrates that the ΔTEC$_{MC}$ are functions of the flare class and eruption location on the solar disc, which can be written as

$$\Delta TEC_{MC} = 0.75\ C_f \cos\theta \qquad (8)$$

where ΔTEC$_{MC}$ is the maximum increased TEC in TECu observed in the midday region and C_f denotes the flare class in term of the X class unit.

[16] In Figure 3b, the regression analysis for the whole data set produces the correlation coefficient between x:flare class in X-ray radiation and y:rTEC$_{MC}$ as 0.673 and indicates that the fitted regression line rTEC$_{MC}$ = 0.243 + 0.056 X-ray explains only 45.33% of the variation of rTEC$_{MC}$. However, after removing the outlier, the extreme large rTEC$_{MC}$ of the X17.2 flare, the correlation coefficient between flare class and rTEC$_{MC}$ is enhanced to be 0.751. If we remove one more influential observation with the X20 flare, the related correlation coefficient becomes as high as 0.917, which implies a strong linear association between flare class and rTEC$_{MC}$.

[17] In Figure 3c, the regression analysis produces 95% confidence intervals for the correlation coefficient between x:the maximum time rate of change in X-ray radiation (rX-ray$_M$) and y:rTEC$_{MC}$ as (−0.254, 0.810) and

(−0.144, 0.871) based on the whole data set and the data set without the outlier, the extreme large $rTEC_{MC}$, of the X17.2 flare, respectively. This means that $rX\text{-}ray_M$ and $rTEC_{MC}$ may not be linearly correlated. However, after removing one more influential observation with $rTEC_{MC}$ of the M9.3 flare, the regression analysis based on the remaining nine pairs of data indicates that the fitted regression line $rTEC_{MC} = 0.292 + 43.423\, rX\text{-}ray_M$ explains 75.27% of the variation of $rTEC_{MC}$. Moreover, the related 95% confidence intervals for the correlation coefficient between the two quantities is given by (0.573, 0.964), which indicates a moderate to strong linear association between $rX\text{-}ray_M$ and $rTEC_{MC}$.

[18] Both the $rTEC_M$ and $rTEC_{MC}$ of the X20 flare are much less than the linear prediction (Figure 3b), which might result from that the flare erupted gradually having a very small $rX\text{-}ray_M$ (see Table 1 and Figure 3c). On the other hand, although the associated $rX\text{-}ray_M$ is rather large, the $rTEC_M$ and $rTEC_{MC}$ of the M9.3 flare are much less than the prediction, which is possibly due to the relative small flare class (i.e., flare radiations) (Figure 3c). By contrast, Figures 3b and 3c display that the $rTEC_M$ and $rTEC_{MC}$ of the X17.2 flare are much greater than the predications. It can be seen in the X17.2 flare that occurred on 28 October 2003, both the observed ΔTEC_M and $rTEC_M$ yield the greatest values among the 11 events. Note that there are double sudden-increases (peaks) in the rTEC at about 1103 and 1105 UT, while the rX-ray radiation only has a single peak at about 1105 UT (Figure 2b). It is interesting to find that the EUV radiation in the X17.2 flare also has double peaks at about 1103 and 1105 UT [see *Tsurutani et al.*, 2005, Figure 3]. The double peaks in the rTEC confirm both the X-ray and EUV radiations to be important. It might be the enormous EUV radiations significantly contribute to the ΔTEC_M and $rTEC_M$ of the X17.2 flare (B. T. Tsurutani, private communication, 2005). Nevertheless, after removing the outliers of the X20, X17.2, and M9.3 flares (Figures 3b and 3c), we find that the $rTEC_M$ is a function of the flare class and the time rate of change of flare radiations.

[19] In conclusion, this study shows that the solar disc location of the flare has significant effect to the ionospheric response. The linear relation between the flare X-ray radiations and the cosine-angle-corrected TEC increases suggests that the center-to-limb effect of the flare radiation spectra also exists in the X-ray radiation.

[20] **Acknowledgments.** Data used in this paper are from IGS and Ministry of the Interior of Taiwan. The SOHO EIT images are taken from the SOHO official Web site of http://sohowww.nascom.nasa.gov/. This research was partially supported by the Ministry of Education grant 91-N-FA07-7-4 and National Science Console project, NSC-94-2111-M-008-024-AP5. C. H. Lin is supported in part by the Newkirk Fellowship of the NCAR/HAO and the NASA Sun-Earth Connection Theory Program.

[21] Shadia Rifai Habbal thanks Takeo Kosugi and Manuel Hernandez-Pajares for their assistance in evaluating this paper.

References

Bennett, J. A. (1967), The calculation of Doppler shifts due to a changing ionosphere, *J. Atmos. Terr. Phys.*, *29*, 887.

Davies, K. (1980), Recent progress in satellite radio beacon studies with particular emphasis on the ATS-6 radio beacon experiment, *Space Sci. Rev.*, *25*, 357.

Davies, K. (1990), *Ionospheric Radio*, 580 pp., Peter Peregrinus, London.

Deshpande, S. D., and A. P. Mitra (1972), Ionospheric effects of solar flares -IV. Electron density profiles deduced from measurements of SCNA's and VLF phase and amplitude, *J. Atmos. Terr. Phys.*, *34*, 255.

Donnelley, R. F. (1971), Extreme ultraviolet flash of solar flare observed via sudden frequency deviation: Experimental results, *Solar Phys.*, *20*, 188.

Donnelly, R. F. (1976), Empirical models of solar flare x-ray and EUV emissions for use in studying their E and F region effects, *J. Geophys. Res.*, *81*, 4745.

Hunsucker, R. D. (1991), *Radio Techniques for Probing the Terrestrial Ionosphere*, Springer, New York.

Jones, T. B. (1971), VLF phase anomalies due to a solar X-ray flare, *J. Atmos. Terr. Phys.*, *33*, 963.

Kendall, M., A. Stuart, and J. K. Ord (1977), *The Advanced Theory of Statistics*, vol. I., 4th ed., Library of Congress, London.

Leick, A. (1995), *GPS Satellite Surveying*, 560 pp., John Wiley, Hoboken, N. J.

Liu, J. Y., C. S. Chiu, and C. H. Lin (1996a), The solar flare radiation responsible for sudden frequency deviation and geomagnetic fluctuation, *J. Geophys. Res.*, *101*, 10,855.

Liu, J. Y., H. F. Tsai, and T. K. Jung (1996b), Total electron content obtained by using the global positioning system, *Terr. Atmos. Oceanic Sci.*, *7*, 107.

Liu, J. Y., C. H. Lin, H. F. Tsai, and Y. A. Liou (2004), Ionospheric solar flare effects monitored by the ground-based GPS receivers: Theory and observation, *J. Geophys. Res.*, *109*, A01307, doi:10.1029/2003JA009931.

Mendillo, M., et al. (1974), et al Behavior of the ionospheric F region during the greatest solar flare of August 7, 1972, *J. Geophys. Res.*, *79*, 665.

Mitra, A. P. (1974), *Ionospheric Effects of Solar Flares*, 294 pp., Springer, New York.

Ohshio, M. (1971), Negative sudden phase anomaly, *Nature*, *229*, 239.

Sao, K., M. Yamashita, S. Tanahashi, H. Jindoh, and K. Ohta (1970), Sudden enhancements (SEA) and decreases (SDA) of atmospherics, *J. Atmos. Terr. Phys.*, *32*, 1567.

Sardón, E., A. Rius, and N. Zarraoa (1994), Estimation of the transmitter and receiver differential biases and the ionospheric total electron content from global positioning system observation, *Radio Sci.*, *29*, 577.

Stonehocker, G. H. (1970), Advanced telecommunication forecasting technique, in *Ionospheric Forecasting*, *AGARD Conf. Proc. 29*, edited by V. Agy, pp. 27-1, Advis. Group for Aerosp. Res. and Dev., North Atl. Treaty Org., Brussels.

Tsurutani, B. T., et al. (2005), The October 28, 2003 extreme EUV solar flare and resultant extreme ionospheric effects: Comparison to other Halloween events and the Bastille Day event, *Geophys. Res. Lett.*, *32*, L03S09, doi:10.1029/2004GL021475.

Zhang, D. H., and Z. Xiao (2003), Study of the ionospheric total electron content response to the great flare on 15 April 2001 using the International GPS Service network for the whole sunlit hemisphere, *J. Geophys. Res.*, *108*(A8), 1330, doi:10.1029/2002JA009822.

Zhang, D. H., Z. Xiao, and Q. Chang (2002), The correlation of flare's location on solar disc and the sudden increase of total electron content, *Chin. Sci. Bull.*, *47*, 82–85.

C. H. Chen, Y. C. Chen, T. W. Fang, C. H. Lin, Y. C. Lin, and J. Y. Liu, Institute of Space Science, National Central University, No. 300, Chung-Da Road, Chung-Li 32001, Taiwan. (jyliu@jupiter.ss.ncu.edu.tw)

Y. I. Chen, Institute of Statistics, National Central University, Chung-Li 32001, Taiwan.

J. J. Hwang, Science Education Department, National Museum of Natural Sciences, 1 Guancian Road, Tai-Chung, Taiwan.